Energy Conversion and Management 350 (2026) 120947

Contents lists available at ScienceDirect

Energy Conversion and Management

journal homepage: www.elsevier.com/locate/enconman

Research Paper

Optimal sizing of battery energy storage systems for peak shaving and demand response using a degradation-aware Bayesian Optimization-Mixed-Integer Linear Programming framework

Jiwei Yao [a], Blake Billings [b], Tao Gao [a], John Hedengren [c], Kody M. Powell [a,d,*]

[a] Department of Chemical Engineering, University of Utah, Salt Lake City, Utah 84112, USA
[b] Oak Ridge National Laboratory, Oak Ridge, TN 37830 USA
[c] Department of Chemical Engineering, Brigham Young University, Provo, UT 84604, USA
[d] Department of Mechanical Engineering, University of Utah, Salt Lake City, Utah 84112, USA

ARTICLE INFO

Keywords:
Batteries
Bayesian optimization
Optimal sizing
Energy storage
Energy management

ABSTRACT

The increasing integration of renewable energy and rising electricity demand highlight the importance of battery energy storage systems for peak shaving and demand response. Unlike prior approaches that overlook operational impacts on degradation, this study proposes a Bayesian Optimization–Mixed Integer Linear Programming framework for optimal battery energy storage system sizing. In this framework, Mixed Integer Linear Programming determines short-term scheduling while a calibrated electrochemical model iteratively evaluates degradation. The central hypothesis is that the framework can efficiently identify optimal sizes that yield realistic and economically robust outcomes. The method is tested across three scenarios: peak shaving, peak shaving with energy-reduction demand response, and peak shaving with power-reduction demand response. Results show that the framework converge to the optimum within 20 iterations out of 150 possible sizes. Under baseline conditions, the framework consistently selects the smallest feasible system, minimizing unnecessary degradation costs from oversized storage. Sensitivity analyses reveal that larger systems are favored as demand rates or incentives increase. Comparisons of demand response programs indicate that power-reduction demand response offers greater economic benefits than energy-reduction demand response, although demand savings from peak shaving remain the dominant contributor to overall performance. This study demonstrates that the proposed framework balances computational tractability with degradation fidelity, identifies critical economic thresholds for investment, and offers a practical, flexible tool to guide industrial stakeholders in cost-effective battery energy storage system deployment.

1. Introduction

The global electricity system is undergoing a profound transformation, driven by factors such as population growth [1], economic expansion [2], widespread electrification [3], and the increasing penetration of renewable energy sources [4]. This evolution has resulted in a substantial rise in electricity demand across all sectors. Notably, industrial electricity consumption is projected to increase significantly impacting existing grid infrastructure [5]. The challenges of this transition are further exacerbated by the variability and unpredictability of renewable energy sources like solar and wind which are growing at unprecedented rates [6]. A critical issue in modern energy management is the mitigation of sudden spikes in energy demand, which can compromise the stability of the grid system by increasing the likelihood of system failures and degrading power quality [7]. Demand response (DR) programs have been introduced to alleviate these pressures, allowing consumers to support grid stability by reducing or shifting electricity usage during peak periods in exchange for incentives or time-based pricing [8]. Therefore, peak shaving (PS) is becoming an even more pressing research area. However, effective participation in PS often requires dynamic and flexible load adjustments, which may not be feasible for many end-users. This limitation highlights the growing importance of energy storage systems. Among available technologies, battery energy storage systems (BESSs) stand out as a viable solution due to their scalable capacity, minimal site constraints, and fast response capabilities.

* Corresponding author.
E-mail address: kody.powell@utah.edu (K.M. Powell).

https://doi.org/10.1016/j.enconman.2025.120947
Received 11 July 2025; Received in revised form 4 December 2025; Accepted 11 December 2025
Available online 19 December 2025

In recent years, BESSs have seen growing adoption in residential [9] and utility-scale sectors [10]. However, their use within industrial applications remains relatively limited due to several factors, including diverse load profiles, varying degrees of tolerance to uncertainty, multiple rate structures, and stringent payback requirements [11]. Numerous studies have recently emerged to address these challenges. Billings et al. applied Gaussian process regression (GPR) coupled with Bayesian decision theory to manage BESS operations in industrial settings, explicitly addressing uncertainty in electrical loads [12]. Sanjari et al. developed an analytical closed-form strategy for optimal battery scheduling in energy systems under load demand uncertainty [13]. Carpinelli et al. considered both uncertain electricity prices and load demands for the sizing problem [14]. Hartmann et al. performed an economic analysis involving 21 commercial and industrial load profiles, concluding that cost reduction varies notably with different load profiles [15]. Despite these advancements, determining the appropriate capacity of a BESS for PS remains a critical initial step in industrial applications. An incorrect estimation of the required capacity could transform anticipated benefits into economic disadvantages. An oversized BESS may be economically impractical since capital expenditures and maintenance costs are directly linked to the system size. In contrast, an undersized BESS might fail to deliver the intended advantages [16].

Studies have been conducted to address the challenge of determining the optimal sizing of BESS for PS. However, the size of the BESS is also determined by the operation. In other words, solving the BESS's operation problem is usually required to solve the optimal sizing problem. By building a correlation between the peak demand and energy usage based on the historical load profile, Chua et al. proposed a novel sizing method along with a rule-based control strategy to iteratively obtain the optimal size of the BESS to minimize the electricity bill for commercial and industrial facilities [17]. Alexandre et al. utilized an "extrema" method where the objective function is evaluated for a set of BESS sizes, and BESSs are controlled with a dynamic programming (DP) algorithm [18]. Leadbetter et al. identified the optimal size of the BESS by finding the smallest BESS size that can achieve most of the PS event, which is determined by a manually calculated grid demand threshold without considering battery degradation [19]. By assuming the power capacity is predetermined, Lu et al. proposed a mixed-integer programming (MIP) model to minimize the power fluctuation without considering the BESS's capital cost [20]. Similar approaches have been proposed by Inaolaji et al. with a mixed-integer linear programming (MILP) model [21] and by Martins et al. with a linear programming (LP) model [22], addressing both optimal sizing and optimal operation at once. On the other hand, Wankhade et al. proposed a framework that uses emperor penguin optimization to find the optimal BESS scheduling and uses battle royale optimization for optimal sizing [23]. Other studies also proposed methods to addressing the optimal size for PS with different conditions: uncertainty [14], location [24], and on-site renewable energy generation [25].

Despite these advancements in finding the optimal size for BESS to participate in PS, most of these studies overlook the degradation effect in BESS, which is a growing concern as the Li-ion battery is becoming more and more popular in BESS applications. However, in some studies, the impact of the degradation on the optimal sizing is overlooked. For example, Wankhade et al. only considered the battery's SOC limit [23]. Ke et al. adopted a rule-based strategy to tune the size with consideration of the charge and discharge trigger point [25]. Without consideration of degradation, the size of the BESS might not be optimal, leading to a high payback period, which is not desirable for industrial applications as the cost of degradation is a significant cost driver [26]. Other studies utilized a predefined lifetime to account for the cost, for example Chua et al. [17], and Oudalov et al. [18] using a fixed cycle lifetime. However, the operation affects the Li-ion battery's lifetime [27].

To address this problem, some studies adopted the levelized cost of storage (LCOE) concept to capture the relationship between usage and degradation [28]. For example, Lu et al. integrated the cost of storage into the objective function to factor in the operation's impact on degradation by assuming the BESS will have a depth of discharge at 50 % [20]. Similar methods are also applied in other studies. Shi et al. addressed the battery cost with a fixed marginal cost which is calculated from a fixed cyclelife [29]. Englberger et al. use the ratio between the throughput energy and the expected throughput over the lifetime to reflect the degradation cost [30].

Compared to approaches that rely on a fixed lifespan for calculating BESS degradation expenses, a usage-based cost model more accurately reflects the impact of charging and discharging on system wear. However, this method overlooks a degradation pattern of Li-ion battery: calendar aging. Calendar aging encompasses all mechanisms that degrade a battery cell regardless of charge–discharge cycle, such as the growth of electrode–electrolyte interfaces (SEI). It becomes especially significant in many Li-ion battery applications, where actual operating periods are notably shorter than the intervals of inactivity, such as BESS for PS [33]. To further capture the degradation effects, some studies adopted semi-empirical models. For example, Martins et al. solved the optimal sizing problem by considering both cycle aging and calendar aging. Calendar aging is tracked with a function that respects time and state of charge (SOC) while cycle aging is tracked by usage with a predefined cycle lifetime [22]. Hesse et al. adopted a similar approach to determine the optimal BESS size to minimize the energy cost for a household equipped with PV and BESS [26]. By using a rainfall algorithm and relationship between cyclelife and depth of discharge, Shi et al. is able to calculate a dynamic degradation cost [31]. Padmanabhan et al. extrapolated a cost function based on the changes of SOC and power [32]. Semi-empirical models rely on laboratory data, which narrows their flexibility and realism. The laboratory data are obtained with fixed test protocols that don't reflect real-world operating conditions.

Despite the challenge in capturing the impact of degradation on BESS's size, many studies have recently focused on developing optimal scheduling algorithms that allow the BESS to maximize the economic benefit by providing grid services. For example, by solving a joint optimization problem, BESS is used for frequency regulation, and peak shaving reduced the electricity bill by 11.24 % compared to just peak shaving by 1.76 % or just frequency regulation by 6.77 % [29]. Zhang et al. proposed a two-stage stochastic programming model to further handle the uncertainty [34]. Besides frequency regulation, BESS can also generate extra income by participating in event-based DR programs. Peng et al. proposed an optimized economic operation strategy considering event-based DR incentives and peak load shaving [35]. Elio et al. proposed an optimal sizing strategy considering event-based DR incentives [36]. However, the degradation is captured with a semi-empirical approach accounting for calendar and cycle aging separately. Still, it overlooks how time and usage interact to accelerate overall deterioration.

Though many studies have examined different methods to determine the optimal sizing for peak shaving without a comprehensive method to capture the impact of degradation, limited research has been conducted on optimal sizing for peak shaving and enrollment in event-based DR programs. This study proposes an optimal BESS sizing framework for PS and event-based DR incentives. This paper presents a novel contribution by addressing three critical research gaps that have been neglected in previous studies: 1) the impact of degradation on optimal size, 2) taking into account that the size of BESS is comprised of discrete elements, 3) how incentives and demand rates affect the optimal size. The novelties are summarized below:

1. An optimal sizing framework for BESS to participate in PS and event-based DR program. This framework accounts for the battery degradation by utilizing a calibrated electrochemical model.
2. Demonstration that the demand rate and the load factor determine the optimal size for the PS only scenarios. As the demand rate

increases or the load factor decreases, the optimal size will have a higher power limit.
3. Two kinds of event-based DR programs: 1) energy-reduction DR, and 2) power-reduction DR, are evaluated along with PS. We demonstrated that the economic benefit can be improved by participating in the event-based DR programs. However, demand saving from PS dominates the overall savings. Due to the difference in the calculation of the incentives, the proposed framework responds differently as the demand rate and incentive increase.

The rest of this paper is as follows. The proposed framework is introduced in Section 2. The result of the proposed framework is given in Section 3. Finally, Section 4 concludes this paper.

2. Methods

As shown in Fig. 1, for an undersized BESS, limited capacity constrains PS savings, while an oversized BESS diminishes overall economic benefits due to excessive cycling. To determine the optimal size for BESS considering degradation, this section will introduce the proposed Bayesian Optimization (BO)-MixInteger Linear Programming (MILP) framework. The framework separates operation and degradation to preserve computational tractability: the MILP determines the optimal short-term scheduling, while a calibrated electrochemical model evaluates degradation ex-post. Embedding the full nonlinear electrochemical dynamics directly into the MILP would require solving a Mixed Integer Nonlinear Program (MINLP), which is computationally prohibitive for the problem scale considered. To ensure that degradation feeds back into scheduling decisions, the MILP is re-solved iteratively: at the beginning of each month, the current battery state (SOC and SOH) is updated based on the electrochemical simulation of the previous month, and the MILP is solved again to produce an updated optimal schedule. This monthly coupling allows operational decisions to adapt to progressive degradation while maintaining computational efficiency. Moreover, oversizing is penalized indirectly through the ex-post degradation cost, which reduces the net benefit of such solution. The following three key components within the proposed framework will be demonstrated: 1) the BO, 2) the electrochemical battery model, and 3) the optimal scheduling algorithm.

2.1. Optimal sizing with Bayesian Optimization

As mentioned, the operation will affect the optimal size of BESS. Therefore, in this study, a BO-MILP framework is proposed to separate the whole problem into optimal sizing and operation. The proposed framework is demonstrated in Fig. 2. By building a surrogate for the objective function using a Bayesian machine learning technique, GPR, and then using an acquisition function to decide where to explore, BO provides an effective approach to find the optimal solution [37]. In this study, to reflect the real-world BESS sizing constraints, the BESS's size is characterized by two parameters: 1) Maximum Power (P_{max}) and 2) Time Duration (t_{max}) when discharged at P_{max}. Moreover, P_{max} and t_{max} are not continuous variables due to cell and pack design limitations. Therefore, in this study, P_{max} ranges from 100 kW to 3000 kW with 100 kW steps, and t_{max} ranges from 2 h to 10 h with 2 h steps, which covers a total of 150 different sizes ranging from 200kWh (100 kW with 2 h duration) to 30MWh (3000 kW with 10 h duration). The BO-MILP framework will take the facility load profiles, BESS cost data, electricity rate, event-based DR incentives, and corresponding signals to determine the optimal size. Indeed, the search space, which contains 150 different sizes, is limited, and other optimization techniques such as enumerative search could be applied. However, in this study, the evaluation process is computationally intensive, as each candidate requires solving a MILP and simulating with a calibrated electrochemical model. BO can significantly reduce the number of required evaluations by strategically selecting promising candidates through its surrogate model and acquisition function [37].

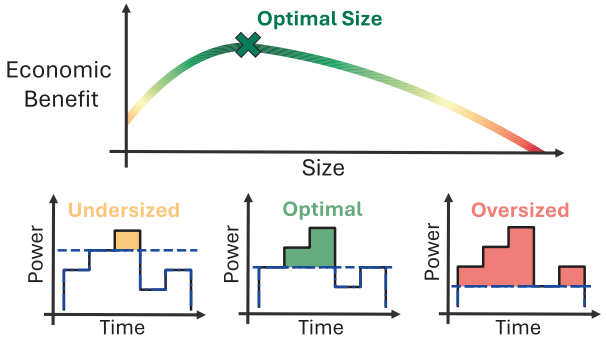

Fig. 1. Finding the optimal size to maximize the economic benefit of the BESS with consideration of degradation.

The whole process is described in Fig. 2, in which it starts with n initial sizes ($(P_{max,1}, t_{max,1})$, $(P_{max,2}, t_{max,2})$, …, $(P_{max,n}, t_{max,n})$) which are randomly drawn from the BESS's design space. For each size, the BESS's operation is determined by solving a MILP to minimize the cost, and then the optimal schedule is simulated with an electrochemical battery model to capture the interaction between operation and degradation. After simulation for a period T, which covers m months, ($T=\{1,2,3,\ldots,m\}$), the objective function for BO (Eq. (1) is evaluated and used to update the GPR-based surrogate model (f) which builds a relationship between the input space (P_{max} and t_{max}) and the BO's objective function's value. In this study, total cost of saving for a period T (TCS_T) is used as the BO's objective value, which is calculated with the demand saving in month m due to reduced peak power demand (S_m^{kw}), usage saving in month m due to on-peak and off-peak electricity rate difference (S_m^{kwh}), incentives in month m due to response to the DR event, operation and maintenance cost (C_{OM}), and degradation cost (C_T^{BESS}). Three inflation factors are added for adjusting utility cost (i_e) [38], operation and maintenance costs (i_o) [38], and normal inflation (i_n) [39]. For a Li-ion battery, the battery needs to be replaced once the state of health drops below 80 %. Therefore, the cost of degradation is calculated with the BESS's state of health at the end of period T (SOH_T) using Eq. (2). The capital expenditures (CAPEX) for the BESS is calculated from existing literature [40]. After updating the GPR-based surrogate model, the evaluated BESS's size has the highest BO's objective value (TCS^*_T) and is denoted as $P^*_{\max}$ and $t^*_{\max}$. If the TCS^*_T value remains the same for consecutive k times exploration, then the corresponding BESS's size is the optimal size. Otherwise, the next step will be generating the next size to be explored. An acquisition function is a mathematical tool used to guide the selection of the next sampling point. The acquisition function can guide the search efficiently by suggesting promising sizes and reducing the number of function evaluations needed to find the optimal size. There are three common acquisition functions: 1) Expected Improvement, 2) Upper Confidence Bound, and 3) Probability of Improvement (PI). Probability of Improvement is chosen in this study because of its simplicity and risk-averse nature, making it ideal when quick, reliable incremental improvements are preferred over riskier exploratory moves. Therefore, the candidate BESS size to be explored can be acquired by maximizing Eq. (3).

$$\mathrm{TCS}_T = C_T^{BESS} + \sum_{m\in T} \frac{\left(S_m^{kW} + S_m^{kWh} + I_m^{DR}\right)(1+i_e)^{\frac{m}{12}} - C_{\mathrm{OM}}(1+i_o)^{\frac{m}{12}}}{(1+i_n)^{\frac{m}{12}}} \quad (1)$$

$$C_T^{BESS} = CAPEX^{BESS} \times \frac{100\% - SOH_T}{100\% - 80\%} \quad (2)$$

$$\mathrm{PI}(P,t) = Pr\left(f(P,t) > TCS_T^*\right) \quad (3)$$

In this study, the initial size, n, is set to be 10 to ensure the initial points cover a broad design space. The surrogate model was then iteratively

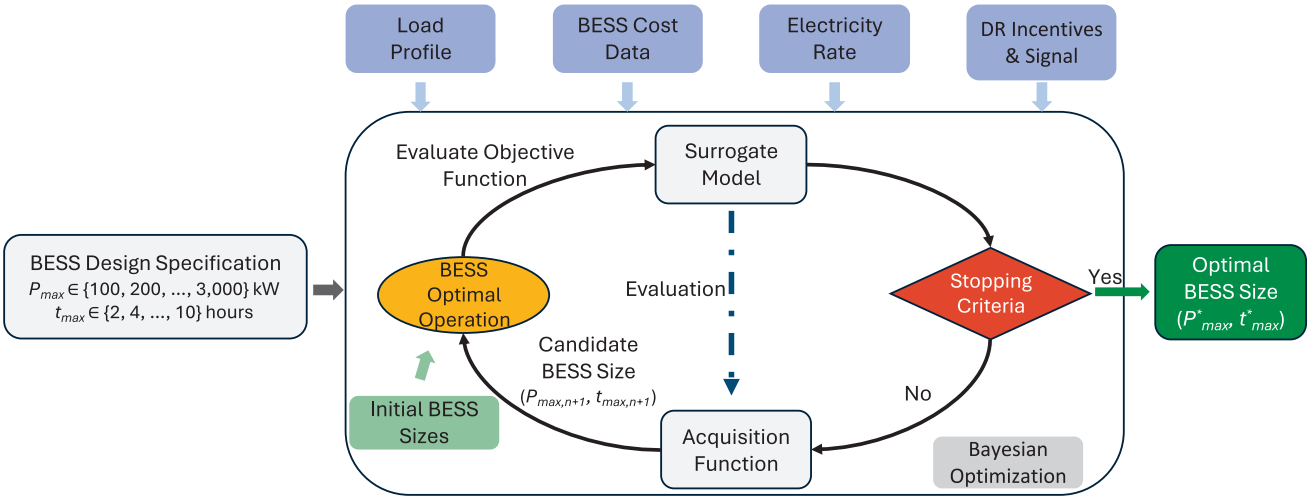

Fig. 2. Workflow of the proposed BO-MILP framework used to find the optimal size.

updated with new evaluations, and the process was terminated after the best objective value did not improve for three consecutive iterations. Given the finite and low-dimensional design space of 150 sizes, this strategy reduces the risk of entrapment in suboptimal regions.

2.2. Optimal operation with Mixed-Integer Linear Programming problems

Unlike residential consumers, which are usually billed by their electricity usage, industrial consumers are generally billed for energy and peak demand. The peak demand depends on the average value of the highest electricity consumption over a defined time interval during a billing period (usually 1 month). Therefore, for a month m, the electricity bill (C_m) for an industrial consumer without BESS is calculated using Eq. (4).

$$C_m = \sum_{n}^{N} \sigma_{m,n}^{kWh} P_{m,n}^{load} \Delta t + \sigma_m^{kW} P_m^{PD} \tag{4}$$

where $\sigma_{m,n}^{kWh}$ is the energy price at time n in month m, $P_{m,n}^{load}$ is the power that the industrial facility draws from the grid, Δt is the duration, σ_m^{kW} is the demand rate in month m, the P_m^{PD} is the peak demand for month m. By installing a BESS that is dedicated to peak shaving, the P_m^{PD} can be reduced to $P_m^{BESS,PD}$ by solving the optimization problem (Eqs. (5)–(10)).

$$\min P_m^{BESS,PD} \sigma_m^{kW} \tag{5}$$

$$P_{m,n}^{load} + P_{m,n}^{BESS,Ch} - P_{m,n}^{BESS,Dis} = P_{m,n}^{BESS,load} \ \forall n \tag{6}$$

$$P_{m,n}^{BESS,load} \times s_{m,n}^{peak} \leqslant P_m^{BESS,PD} \ \forall n \tag{7}$$

$$E_{m,n}^{BESS} + P_{m,n}^{BESS,Ch} \times \Delta t \times \eta^{RT} - P_{m,n}^{BESS,Dis} \times \Delta t = E_{m,n+1}^{BESS} \ \forall n \tag{8}$$

$$SOC_{\min} \leqslant \frac{E_{m,n}^{BESS}}{C^{BESS} \times SOH_m} \leqslant SOC_{\max} \ \forall n \tag{9}$$

$$0 \leqslant P_{m,n}^{BESS,Ch}, P_{m,n}^{BESS,Dis} \leqslant P_{\max}^{BESS} \ \forall n \tag{10}$$

where $P_{m,n}^{BESS,Ch}$ is the BESS's charging power, $P_{m,n}^{BESS,Dis}$ is the BESS's discharging power, $P_{m,n}^{BESS,load}$ is the net industrial load, $s_{m,n}^{peak}$ is a binary variable to determine if time n in month m is in peak hours, $E_{m,n}^{BESS}$ is the stored energy, η^{RT} is the round-trip efficiency, C^{BESS} is the total capacity of BESS, SOH_m is the state of health at the beginning of month m, P_{max} is the maximum power for charging and discharging. By solving the optimization problem monthly with updated SOH, a desired peak demand with BESS is calculated and used as a threshold in a rule-based control strategy to manage the charging and discharging behavior of the BESS. During on-peak hours, the BESS discharges if the industrial load exceeds $P_m^{BESS,PD}$, and charges if the industrial load is lower than $P_m^{BESS,PD}$. The discharging and charging power can be calculated using Eq. (11).

$$\text{On - peak}: P_{m,n}^{BESS} = P_m^{BESS,PD} - P_{m,n}^{load} \ \forall n \tag{11}$$

Therefore, the new electricity bill with BESS focusing on peak shaving for month m can be calculated using Eq. (12).

$$C_m^{BESS} = \sum_{n}^{N} \sigma_{m,n}^{kWh} P_{m,n}^{BESS,load} \Delta t + \sigma_m^{kW} P_m^{BESS,PD} \tag{12}$$

By enrolling in event-based DR programs, a BESS can unlock extra income, but dedicated control strategies are needed to maximize returns while it handles both PS and DR. Utilities generally structure event-based DR incentives in two ways [8]:

1. **Energy–reduction DR** rewards sites for cutting total energy usage over the event window, independent of instantaneous power demand.
2. **Power–reduction DR** pays only when the facility trims the power demand by a specified kW amount during the event.

For the energy-reduction DR, the corresponding optimization problem can be formulated as Eqs. (13)–(19).

$$\min P_m^{BESS,PD} \sigma_m^{kW} - \sigma^{DR,kWh} \sum_{j \in J} s_{m,j}^{DR} \sum_{n \in T_j^{DR}} P_{m,n}^{BESS,Dis} \Delta t \tag{13}$$

$$P_{m,n}^{load} + P_{m,n}^{BESS,Ch} - P_{m,n}^{BESS,Dis} = P_{m,n}^{BESS,load} \ \forall n \tag{14}$$

$$P_{m,n}^{BESS,load} \times s_{m,n}^{peak} \leqslant P_m^{BESS,PD} \ \forall n \tag{15}$$

$$P_{m,n}^{BESS,Ch} \leqslant P_{\max}^{BESS} \left(1 - s_{m,j}^{DR}\right) \ \forall n \in T_j^{DR}, \forall j \in J \tag{16}$$

$$E_{m,n}^{BESS} + P_{m,n}^{BESS,Ch} \times \Delta t \times \eta^{RT} - P_{m,n}^{BESS,Dis} \times \Delta t = E_{m,n+1}^{BESS} \ \forall n \tag{17}$$

$$SOC_{\min} \leqslant \frac{E_{m,n}^{BESS}}{C^{BESS} \times SOH_m} \leqslant SOC_{\max} \ \forall n \tag{18}$$

$$0 \leqslant P_{m,n}^{BESS,Ch}, P_{m,n}^{BESS,Dis} \leqslant P_{\max}^{BESS} \ \forall n \tag{19}$$

Compared to the previous optimization problem designed for PS, the

objective function contains two terms: the first term represents the new demand cost, and the second one represents the collected incentive by participating in the event-based DR program. $\sigma^{DR,kWh}$ is the DR's incentive with a unit in \$/kWh. J represents the number of DR happening within month m. T_j^{DR} is the subset of time in which the jth DR event happens. A constraint (Eq. (16)) is added to ensure the BESS is not charging if it decides to participate in the jth DR event.

In contrast to the energy-reduction DR, in which the incentive is calculated based on the reduced energy usage, in the power-reduction DR, the incentive is calculated based on the reduced power and the number of responses to the DR signals. Therefore, the above optimization problem can be formulated as Eqs. (20)–(27).

$$\min P_m^{BESS,PD}\sigma_m^{kW} - \sigma^{DR,kW}P^{BESS,DR}\sum_{j\in J} s_{m,j}^{DR} \tag{20}$$

$$P_{m,n}^{load} + P_{m,n}^{BESS,Ch} - P_{m,n}^{BESS,Dis} = P_{m,n}^{BESS,load} \ \forall n \tag{21}$$

$$P_{m,n}^{BESS,load} \times s_{m,n}^{peak} \leqslant P_m^{BESS,PD} \ \forall n \tag{22}$$

$$P_{m,n}^{BESS,Ch} \leqslant P_{\max}^{BESS}\left(1 - s_j^{DR}\right) \ \forall n \in T_j^{DR}, \forall j \in J \tag{23}$$

$$P_{m,n}^{BESS,Dis} \geqslant s_j^{DR}P^{BESS,DR} \ \forall n \in T_j^{DR}, \forall j \in J \tag{24}$$

$$E_{m,n}^{BESS} + P_{m,n}^{BESS,Ch} \times \Delta t \times \eta^{RT} - P_{m,n}^{BESS,Dis} \times \Delta t = E_{m,n+1}^{BESS} \ \forall n \tag{25}$$

$$SOC_{\min} \leqslant \frac{E_{m,n}^{BESS}}{C^{BESS} \times SOH_m} \leqslant SOC_{\max} \ \forall n \tag{26}$$

$$0 \leqslant P_{m,n}^{BESS,Ch}, P_{m,n}^{BESS,Dis} \leqslant P_{\max}^{BESS} \ \forall n \tag{27}$$

The first term in the objective function represents the cost of the new demand cost for month m, while the second term represents the incentives. $\sigma^{DR,kW}$ is the DR's incentive price with a unit in \$/kW per participation. During the jth DR event, two constraints are added to ensure the BESS only discharges at $P^{BESS,DR}$ which is a predetermined power determined by the facility.

2.3. Electrochemical battery model

By solving the corresponding MILP problem, the operation of the BESS can be determined. To capture the operation's impact on degradation, an electrochemical battery model is introduced to simulate the electrochemical behavior of the Li-ion battery. Electrochemical battery model that resolves ion transport, electrode kinetics, and potential fields and can describe degradation in real-time. Here, we use a pseudo-2D model that explicitly includes two key aging pathways: solid-electrolyte interphase growth and irreversible lithium plating [41]. In this study, the degradation rate is calibrated according to a report which states that for Li-ion battery with lithium nickel manganese cobalt as cathode material, the battery can last for 13 years during storage and has a cyclelife of 1520 cycles [40]. This study follows calibration procedures as described in [42]. The electrochemical model is chemistry-agnostic and can be recalibrated by updating cell-specific parameters (e.g., kinetics, transport, aging coefficients), enabling the BO-MILP framework to be applied to other battery cell types.

3. Result and discussion

The electricity rate schedule used in this study is shown in Table 1. As for the energy-reduction DR, the incentive is priced at \$2/kWh [43], while the power-reduction DR is priced at \$100/kW-Year [44]. For the energy-reduction DR, the signal is determined by flex alert history in 2022 sent by CAISO, which has a total of eleven events annually with an average duration of around 5 h [45]. On the other hand, in the power-reduction DR, the signal is determined by the DR program offered by Rocky Mountain Power, which has eight events annually with an average duration of around 30 min [46]. For the power-reduction DR program, at the beginning of each calendar year y, the facility must decide how much power it will participate with in the program. Utility companies typically require the power reduction to last at most 4 h. Therefore, at year y, $P^{BESS,DR}$ is calculated using Eq. (28).

Table 1
The facility's electricity rate schedule.

	On-peak[1]	Off-peak[2]
Demand Rate (\$/kW-Month)	16.61	0.00
Usage Rate (¢/kWh)	5.15	2.62

$$P^{BESS,DR} = \min\left(\frac{\mathrm{P_{max}} \times t_{max} \times SOH_y \times (\mathrm{SOC_{max}} - \mathrm{SOC_{min}})}{T_{DR}}, \mathrm{P_{max}}\right) \tag{28}$$

where SOH_y is the state of health at year y, T_{DR} is the maximum duration for the DR, which is 4 h, and SOC_{max} and SOC_{min} are the upper and lower limit of the state of charge, respectively.

1. From 6 am to 9 am, from 6 pm to 10 pm except on weekends in October – May (winter schedule), and from 3 pm to 10 pm except on weekends in June – September (summer schedule).
2. From 10 pm to 6 am and 9 am to 6 pm in October to May (winter schedule), and from 10 pm to 3 pm in June to September (summer schedule), with all hours on weekends being off-peak year-round.

Due to the variation of monthly electricity usage, distribution of DR events, and nonlinear degradation of the BESS, the BO will try to maximize the total cost of saving of the BESS in the first year (TCS@1year). The BO will stop running if the optimal objective value is not improved for three consecutive explorations. Then, the optimal BESS size will be simulated until its end-of-life when its SOH drops below 80 %. The overall economic benefit of BESS that can be generated within its lifespan can be captured by the net present value (NPV) which is calculated using Eq. (29).

$$\mathrm{NPV} = \mathrm{CAPEX} + \sum_{m=1}^{m=m_{EOL}} \frac{\left(S_m^{kW} + S_m^{kWh} + I_m^d\right)(1+i_e)^{\frac{m}{12}} - C_{\mathrm{OM}}(1+i_o)^{\frac{m}{12}}}{(1+i_n)^{\frac{m}{12}}} \tag{29}$$

Because the degradation is related to the operation, using Eq. (30), an equivalent annual annuity (EAA) is adopted to compare BESS with different lifetimes.

$$\mathrm{EAA} = \mathrm{NPV} \times \frac{i_n}{1-(1+i_n)^{-\frac{m}{12}}} \tag{30}$$

Internal return rate (IRR) is also a popular metric for comparing economic performance between different projects. IRR is calculated using Eq. (31).

$$0 = \sum_{m=1}^{m=m_{EOL}} \frac{\left(S_m^{kW} + S_m^{kWh} + I_m^d\right)(1+i_e)^{\frac{m}{12}} - C_{\mathrm{OM}}(1+i_o)^{\frac{m}{12}}}{(1+IRR)^{\frac{m}{12}}} - CAPEX \tag{31}$$

The proposed BO-MILP framework will be evaluated with three scenarios: PS, PS and energy-reduction DR, and PS and power-reduction DR. The result for PS with different pricing and load profiles is demonstrated in Section 3.1. Section 3.2 and Section 3.3 present the results for PS and energy-reduction DR, and PS and power-reduction DR, respectively.

3.1. Result and discussion for peak shaving

Load factor is a measure of how efficiently electrical power is being used over a period and is calculated using Eq. (32).

$$\text{Load Factor} = \frac{P_{Average}}{P_{Peak}} \tag{32}$$

where $P_{average}$ represents the average power during the on-peak hours, calculated by dividing the total energy consumption during the on-peak hours by the total duration of those hours. P_{peak} is the maximum demand observed during the on-peak period. The BO-MILP is applied to an industrial site (site A) with an average load factor of 0.81.

Given the electricity rate schedule and load profile, after testing 16 different sizes, the proposed method determined that the optimal size of BESS has a maximum power at 100 kW with a duration of 2 h, as shown in Fig. 3. This figure presents the predicted TCS@1year for different sizes by utilizing the surrogate model within the BO. It is worth noting that the values of TCS@1year across all 150 sizes are negative because the Li-ion battery will undergo a fast degradation at the beginning of its life. However, as seen horizontally in Fig. 3, the BESS will have a better economic performance with a short duration even with the same maximum power limit. As shown in Fig. 4a, as the duration increases from 2 h to 4 h, the BESS can generate more demand savings. However, as the duration further increases, the benefit is saturated. Because Site A's peak power demand doesn't last long. Therefore, the extra capacity cannot contribute to the PS remaining underutilized. On the other hand, in Fig. 4b, even though the SOH of the BESS increases slightly from 95.95 % with 2 h to 96.82 % with 10 h, for BESS with long duration, the underutilized capacity still undergoes the calendar aging, which significantly reduces the economic benefit. For example, 97.89 % of the lost active Li-ion comes from the calendar loss for the BESS with 10 h duration in contrast to 95.13 % for BESS with 2 h duration. Therefore, given the same maximum power, BESS with a short duration has a better economic performance than that with a long duration. Such trends can also be observed in the vertical direction. The values of TCS@1year gradually decrease as the maximum power increases, given the same duration. To investigate the impact of maximum power on the values of TCS@1year, three BESS sizes with different maximum powers (100 kW, 1000 kW, 2200 kW) and the same duration (2 h) were selected. As shown in Fig. 5a, the demand saving increases with the P_{max} increase. However, according to Fig. 5b, the discharged capacity increased from 173kWh to 10,734kWh by a factor of 62, while the demand saving increased from $17,451 to $146,802 by a factor of 8.4. The difference between these two factors can be explained by Fig. 5c. Compared to reducing the peak to 2441 kW, reducing the peak to 2213 kW and to 1998 kW required shifting more energy from off-peak hours to on-peak hours. For a Li-ion battery, charging and discharging will incur degradation. The total loss of active Li-ion increases from 0.15Ah/cell to 0.17Ah/cell, while the ratio of the loss of active Li-ion caused by the Li plating increases from 4.86 % to 32.59 %, increasing the overall degradation by 14.40 %. Therefore, the BO-MILP will prefer a BESS with a smaller P_{max}. With the optimal BESS size, the BESS can last 139 months, generating an NPV of $85,237 with a corresponding EAA of $8,583/year and an internal return rate of 13.82 %.

To further validate the performance of the proposed method, a sensitivity analysis is conducted with the demand rate increases from $16.61/kW-Month to $49.83/kW-Month. The predicted TCS@1year is normalized in each scenario and demonstrated in Fig. 6. As the demand rate increases, the number of iterations and the tendency to search the lower left corner increases. However, the optimal size remains the same, and the demand rate is increased by 2.5 times. This is because site A has a relatively high load factor every month, meaning saving for PS is limited. Therefore, if the demand rate is not high enough to justify the extra cost brought by the cycle degradation, the proposed method remains choosing the smallest size.

Similar studies are conducted on sites B and C with load factors at

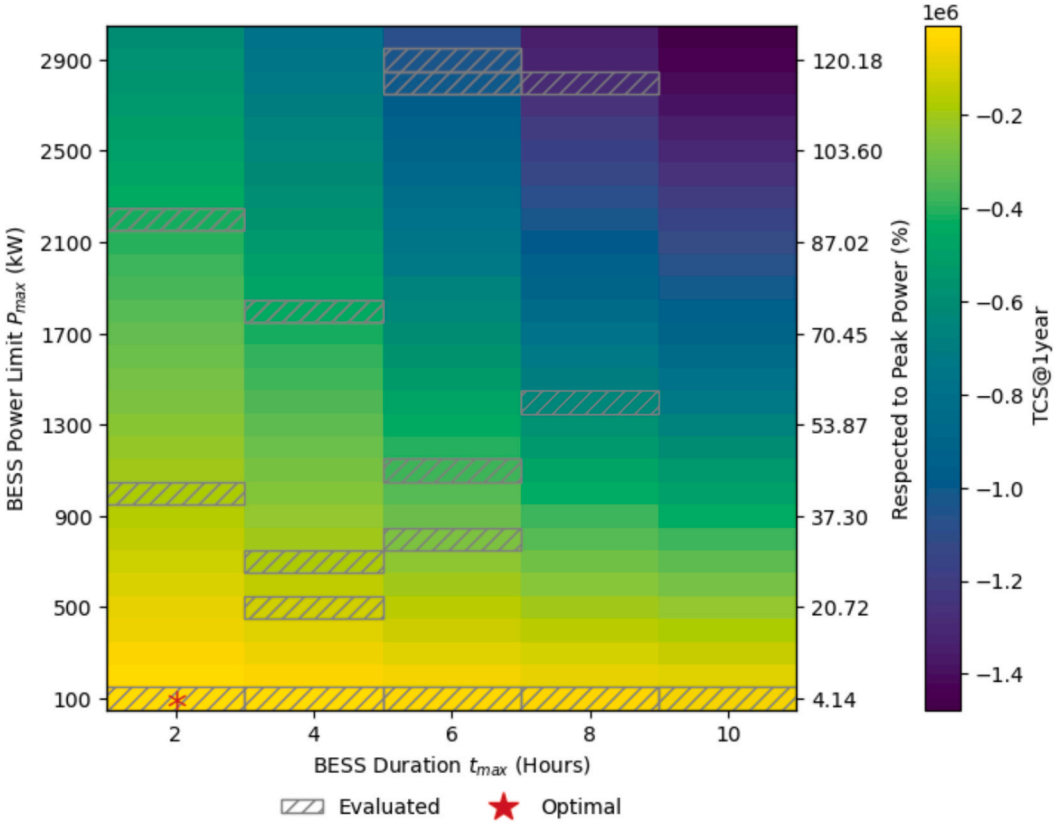

Fig. 3. The predicted TCS@1year using the surrogate model.

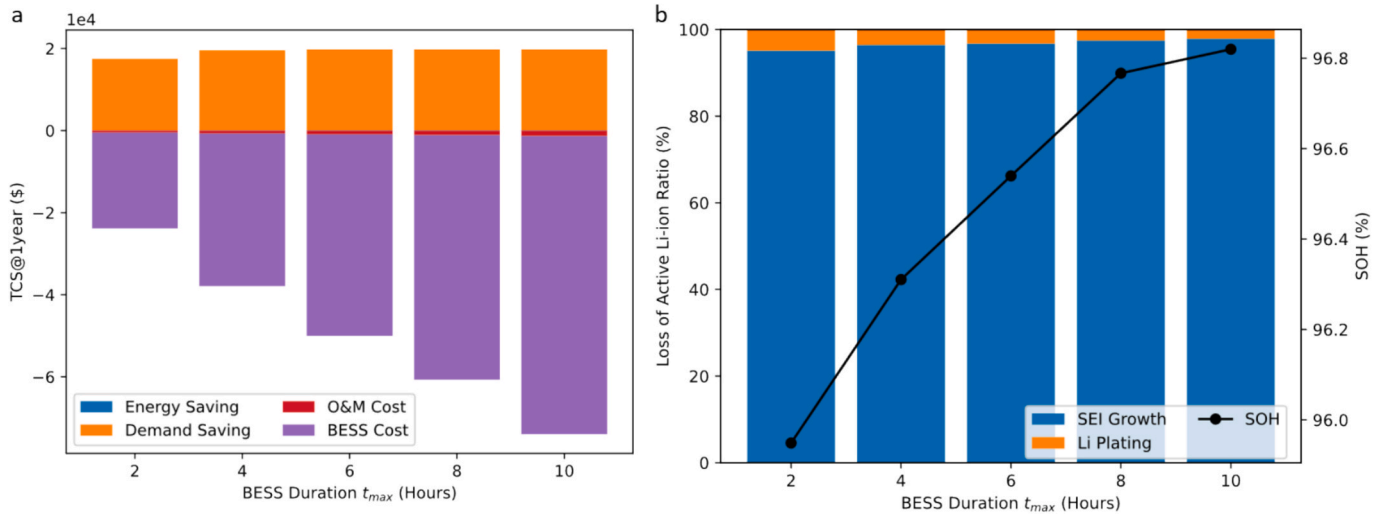

Fig. 4. a) the composition of tcs@1year for bess with the same P_{max} at 100 kW but with different durations. b) As the t_{max} increases, the SOH becomes higher due to some capacity being underutilized.

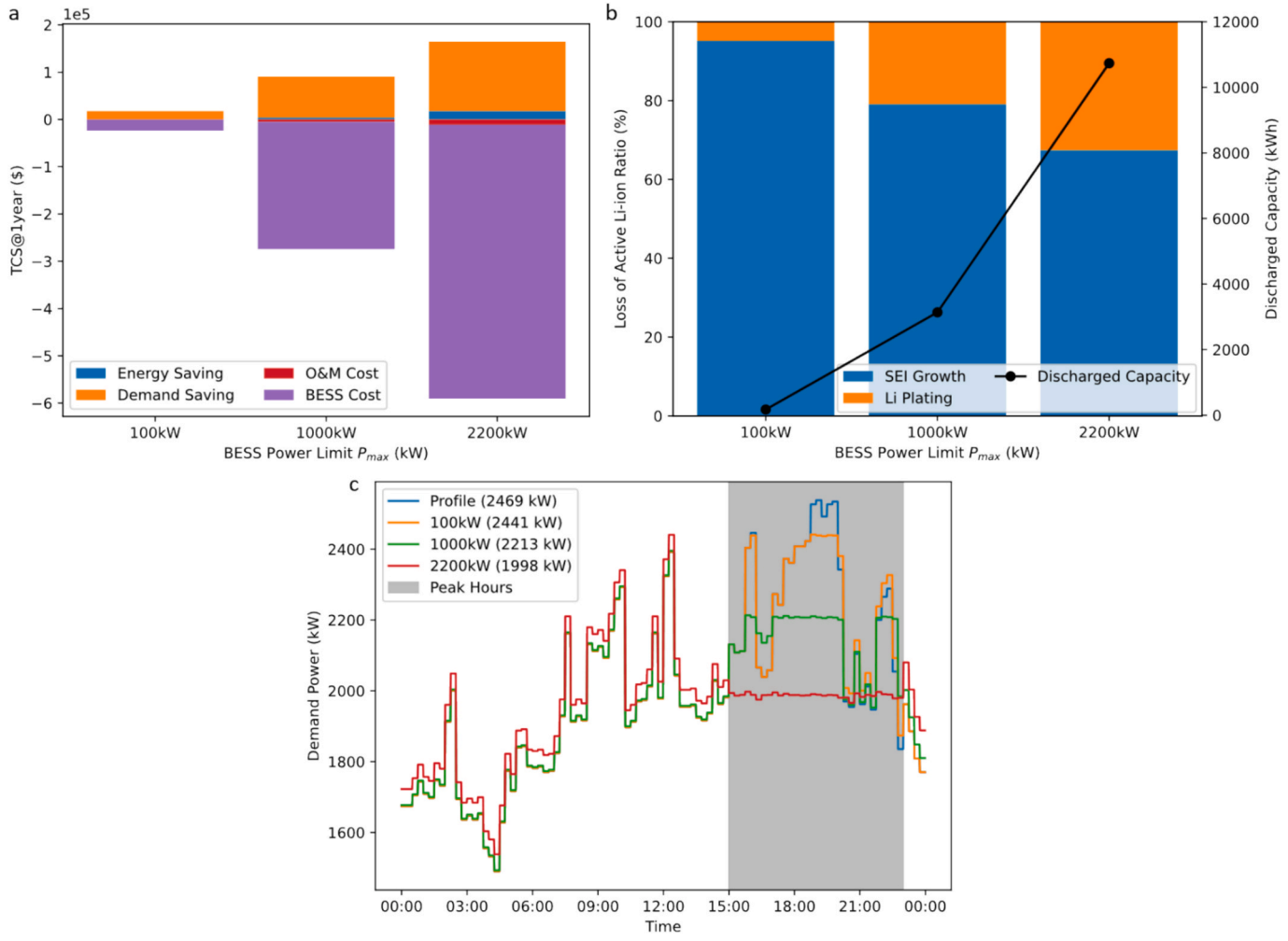

Fig. 5. a) The composition of tcs@1year for bess with the same t_{max} at 2 h but with different $P_{max.}$ As the P_{max} increased, the demand saving also increased proportionally. However, the BESS cost increases much faster due to the b) growing usage. c) With a higher P_{max}, more energy needs to shift from off-peak hours to peak hours, leading to excessive cycling.

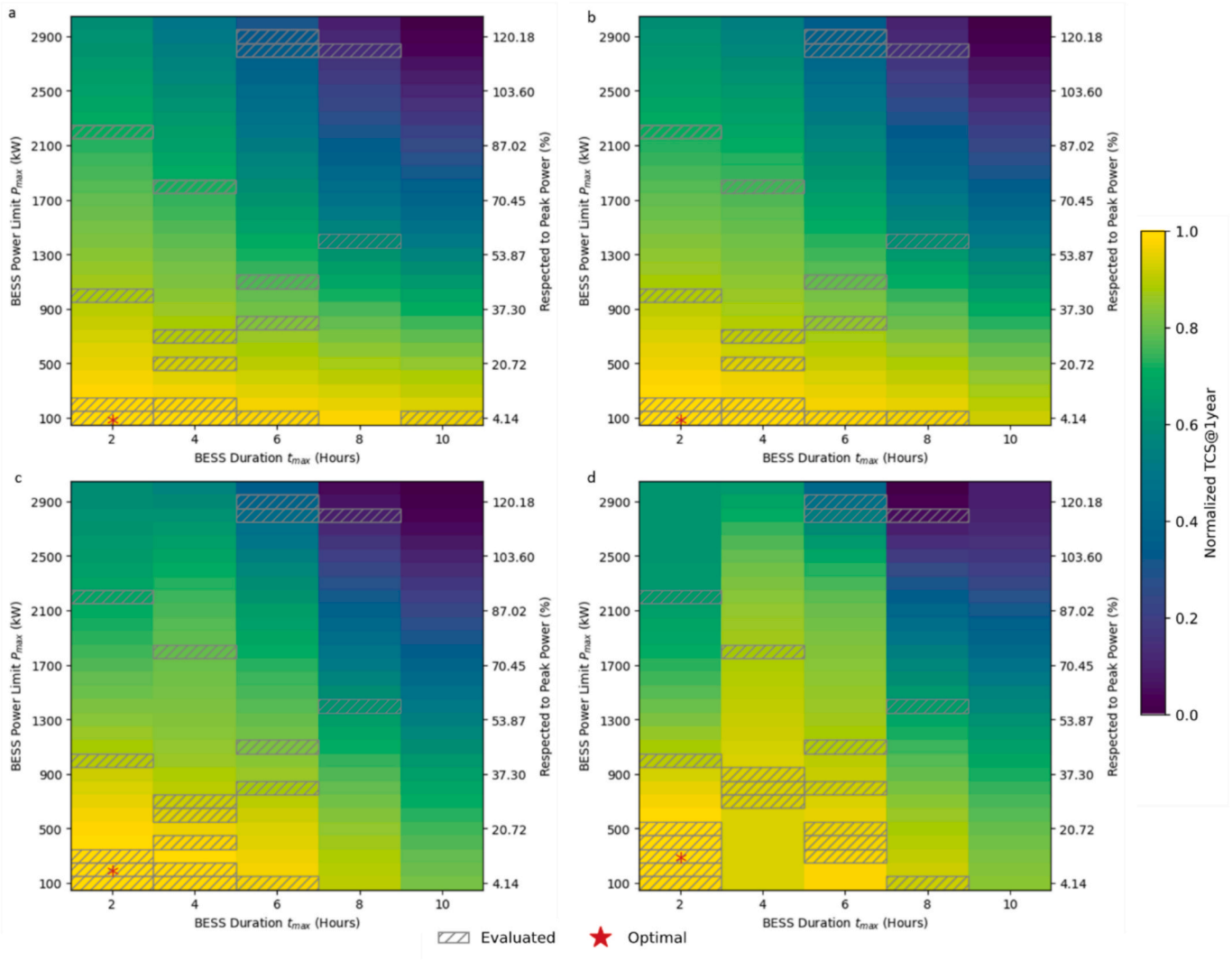

Fig. 6. The predicted normalized TCS@1year and the selected optimal sizes with demand rate at a) $24.91/kW-Month, b) $33.22/kW-Month, c) $41.52/kW-Month, and d) $49.83/kW-Month. As the demand rate increases, the optimal size will have a higher P_{max}.

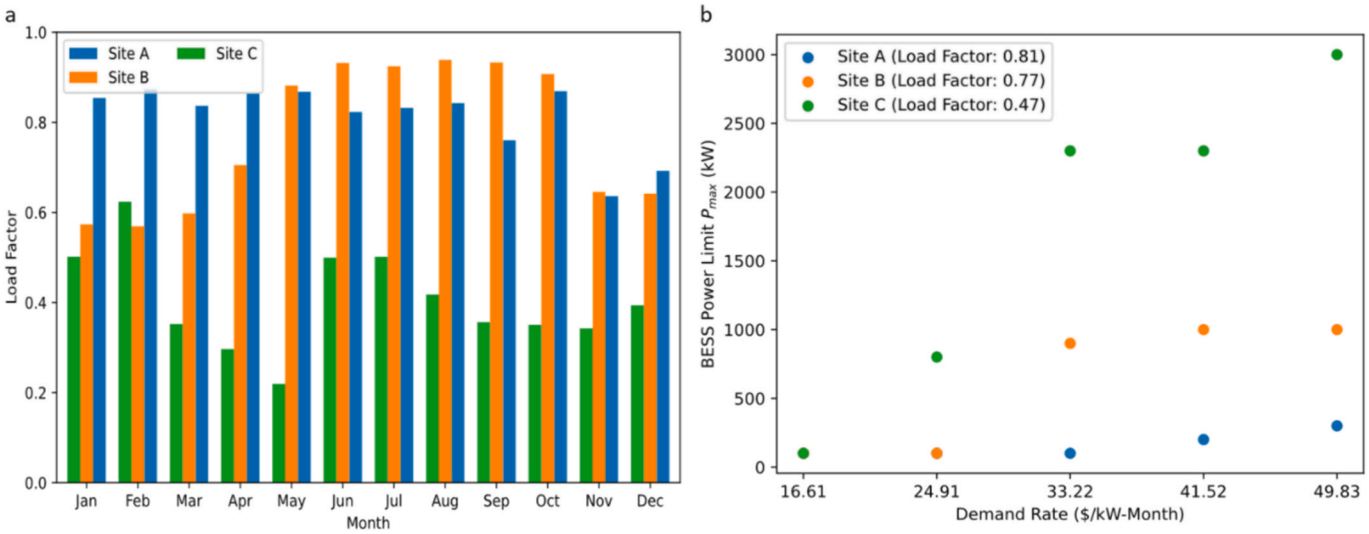

Fig. 7. a) The monthly load factor for site a, site b, and site c. b) The optimal P_{max} for each site under different demand rates.

0.77 and 0.40, respectively, as shown in Fig. 7a. Regardless of the difference in load profile and demand rate, the optimal BESS always results in a duration of 2 h. Given the same capacity (in kWh), a short duration BESS can provide a larger P_{max} than a long duration BESS, leading to more savings by performing PS. However, the load factors affect the optimal P_{max} as the demand rate increases. As shown in Fig. 7b, when compared to site A which has the highest load factor, at site C the P_{max} increases much faster as the demand rate increases, while for site B, the P_{max} increases at a moderate rate. The difference in optimal P_{max} response to demand rate changes can be attributed to the difference in load factor, as demonstrated in Fig. 7a. Generally, a BESS with high P_{max} is preferred for a site with a low load factor and high demand rate. The economic benefits for these three sites with different demand rates are summarized in

Table 2. In all the scenarios, the NPV, EAA, and IRR increase as the demand rate increases. This demonstrates that the proposed BO-MILP framework is able to determine the optimal size of the BESS to maximize the economic benefit from participation in PS under different load profiles and electricity rate schedules by capturing the operation's impact on degradation.

3.2. Result and discussion for peak shaving and energy-reduction demand response

Stacking demand savings and incentives from energy-reduction DR can increase the BESS's economic performance, making it more viable. However, an optimal size needs to be determined to maximize the economic benefit. In this section, with the load profile from site A and the $2/kWh for participating in the energy-reduction DR program, after evaluating 16 different sizes, the BO-MILP method determined that the optimal BESS has a P_{max} at 100 kW and 2 h duration, which is the same size in the PS scenario. In the first year, participation in the energy-reduction DR reduces the demand saving from $17,451 to $16,874. However, such loss is covered by the incentives from the DR program at $2,913, leading to an increase of $2,335 or 13.35 % in the first year. The predicted TCS@1year is shown in Fig. 8. Compared to the previous scenario, BESS with large capacity is not recommended even with the available incentive from the energy-reduction DR. As shown in Fig. 9a, with P_{max} at 100 kW, the PS saving increases as the duration increases from 2 h to 4 h. The demand saving is saturated and remains the same while the duration increases to 6 h and 8 h. However, as the t_{max} increases, the overall capacity increases, and more energy can be discharged during the DR event, leading to increasing incentives. The total saving increases from $19,823 to $30,303. Most of the incremental savings come from the DR program. However, because of the P_{max}, only parts of the capacity can contribute to the demand savings. Indeed, excessive capacity can contribute to the energy-reduction DR generating extra revenue. However, for Li-ion battery, the degradation also comes from the calendar aging. The extra revenue from the DR program is not

Table 2
The economic performance of the BESS with the optimal size under different demand rates.

Demand Rate ($/kW-Month)	NPV($) \| EAA($/year) | IRR(%)		
	Site A	Site B	Site C
16.61	85,237 | 8,583 | 13.82	72,413 | 7,478 | 12.50	91,139 | 9,121 | 14.13
24.91	188,282 | 18,960 | 25.42	169,079 | 17,461 | 23.88	1,371,655 | 140,750 | 23.61
33.22	291,372 | 29,336 | 36.44	1,483,764 | 157,281 | 24.44	3,894,043 | 485,303 | 29.32
41.52	554,679 | 56,917 | 35.56	2,257,953 | 240,948 | 32.08	5,540,547 | 690,501 | 39.39
49.83	876,217 | 89,911 | 36.96	2,943,556 | 314,108 | 40.31	7,187,051 | 895,699 | 49.38

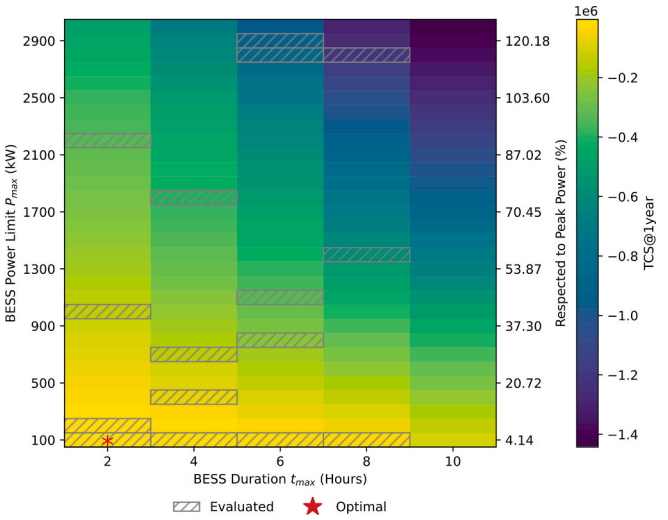

Fig. 8. The predicted TCS@1year for PS and energy-reduction DR using the surrogate model.

enough to cover the cost of degradation. On the other hand, as shown in Fig. 9b, more demand saving and incentive can be collected by increasing the P_{max}, and the total saving increases from $19,823 to $207,111. However, due to the excessive cycle for PS, the BESS cost increases much faster from $23,660 to $527,912. Therefore, the proposed method determined the optimal size of BESS has a P_{max} at 100 kW with a t_{max} at 2 h duration, which can achieve an NPV of $93,698, an EAA of $10,134/year, and an IRR of 16.09 %.

To demonstrate that the proposed framework can work with different demand rates and incentives, a sensitivity analysis is conducted with incentive ranges from $2/kWh to $6/kWh, and demand rate ranges from $16.61/kW-Month to $49.83/kW-Month, leading to a total of 25 different scenarios. The optimal maximum power, duration, and capacity are presented in Fig. 10. In general, as the demand rate and the incentive increase, the proposed method tends to select a BESS with large capacity either by increasing the maximum power, duration, or both to maximize the economic benefit. However, for the scenario with a demand rate of $49.83/kW-Month and an incentive of $2/kWh, the proposed method chooses a larger capacity than the scenario with a demand rate of $49.83/kW-Month and an incentive of $3/kWh. This inconsistency may be caused by the BO process's early termination, leading to a suboptimal result. One-way Analysis of Variance (ANOVA) was conducted on the optimal P_{max} and t_{max}. The result reveals that the demand rate is the dominant factor for the optimal P_{max} and t_{max}. These results correspond to the high percentage of the saving that comes from demand saving, as shown in Fig. 11, wherein in all the scenarios, the demand saving accounts for more than 60 % of the total saving.

3.3. Result and discussion for peak shaving and power-reduction demand response

In this scenario, the objective of the proposed BO-MILP framework is to find the optimal size such that it can maximize the total economic benefit by doing PS along with participation in power-reduction DR. Given the load profile from Site A and real-world DR signal, after evaluating 17 different sizes, the optimal size for performing both PS and power-reduction DR is BESS with P_{max} at 100 kW and duration at 2 h as shown in Fig. 12. With the same size as the previous scenarios, by participating in the power-reduction DR program, in the first year, the total saving is $21,013, which increases by 20.15 % and 6.00 % with respect to the PS scenario and PS energy-reduction DR scenario, respectively. As shown in Fig. 13a, as the duration increases, the demand saving first increases and then saturated. However, unlike the energy-

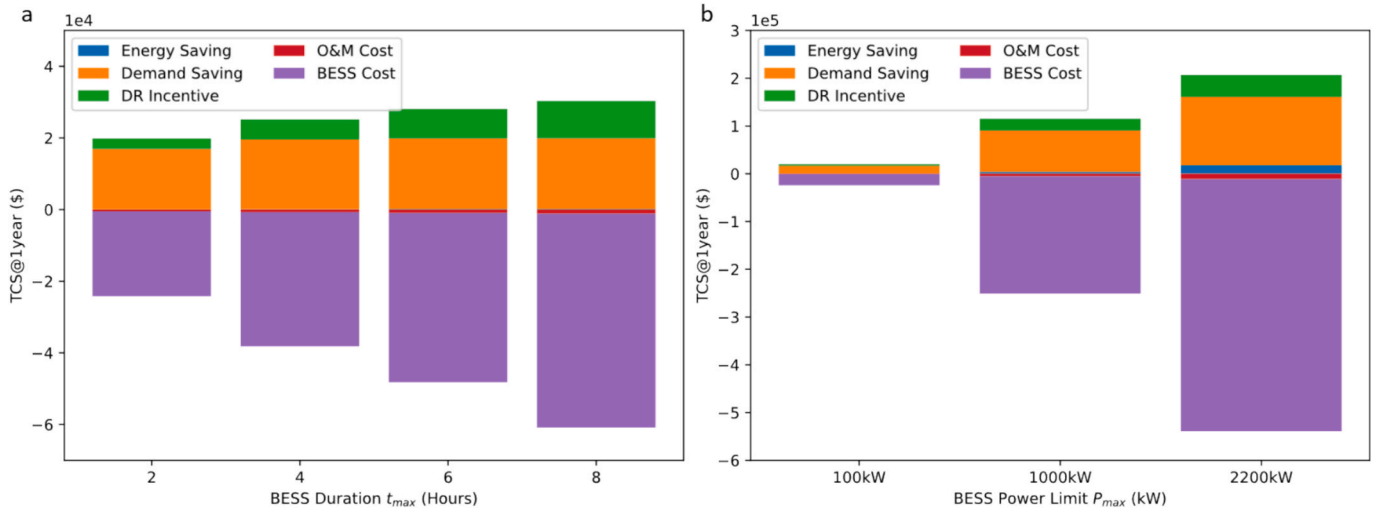

Fig. 9. a) The composition of TCS@1year for BESS with the same P_{max} at 100 kW but with durations ranging from 2 h to 8 h. b) The composition of TCS@1year for BESS with the same t_{max} at 2 h but with P_{max} ranging from 100 kW to 2200 kW.

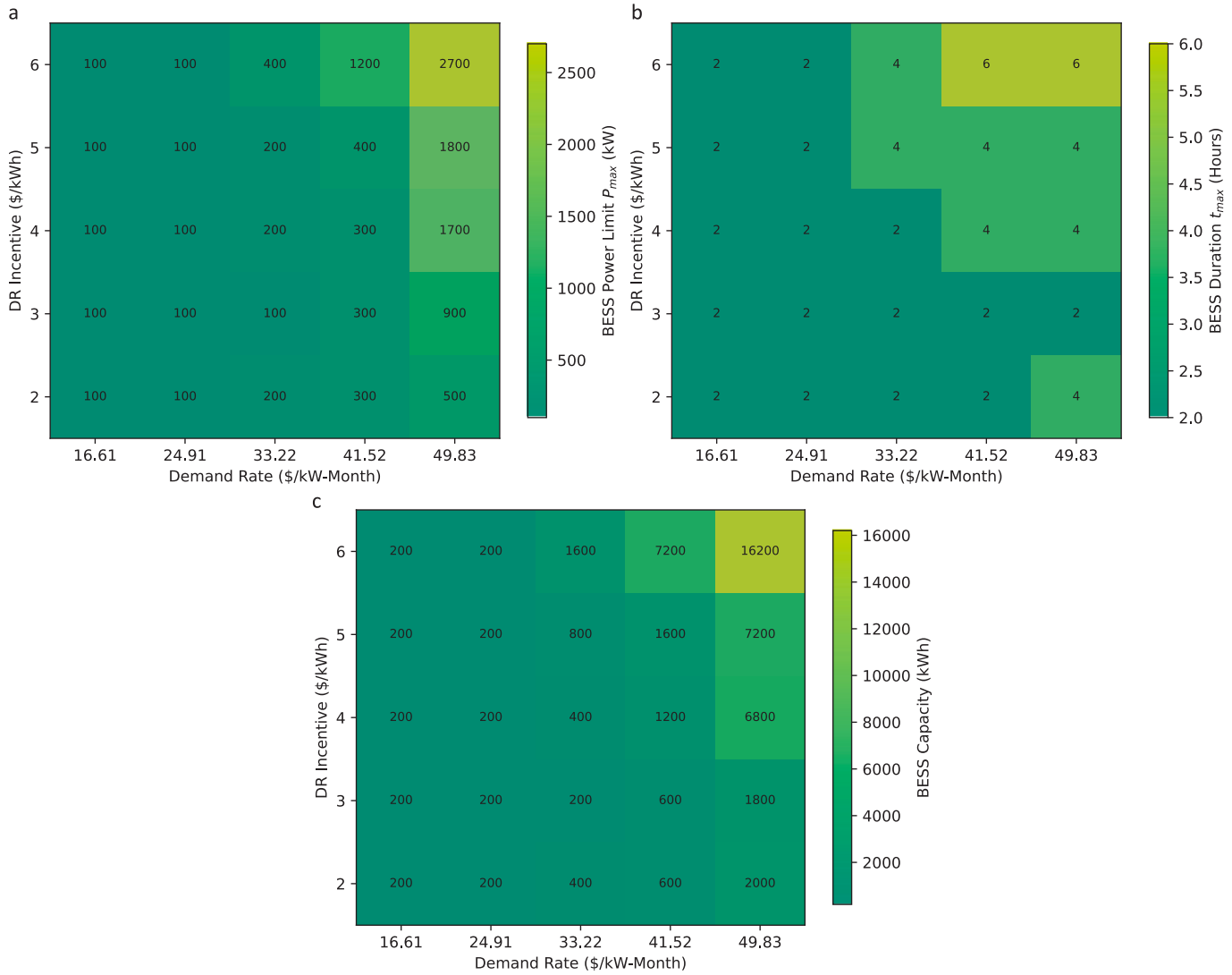

Fig. 10. The optimal a) P_{max}, b) t_{max}, and c) capacity are determined by the BO-MILP framework under different demand rates and DR incentives.

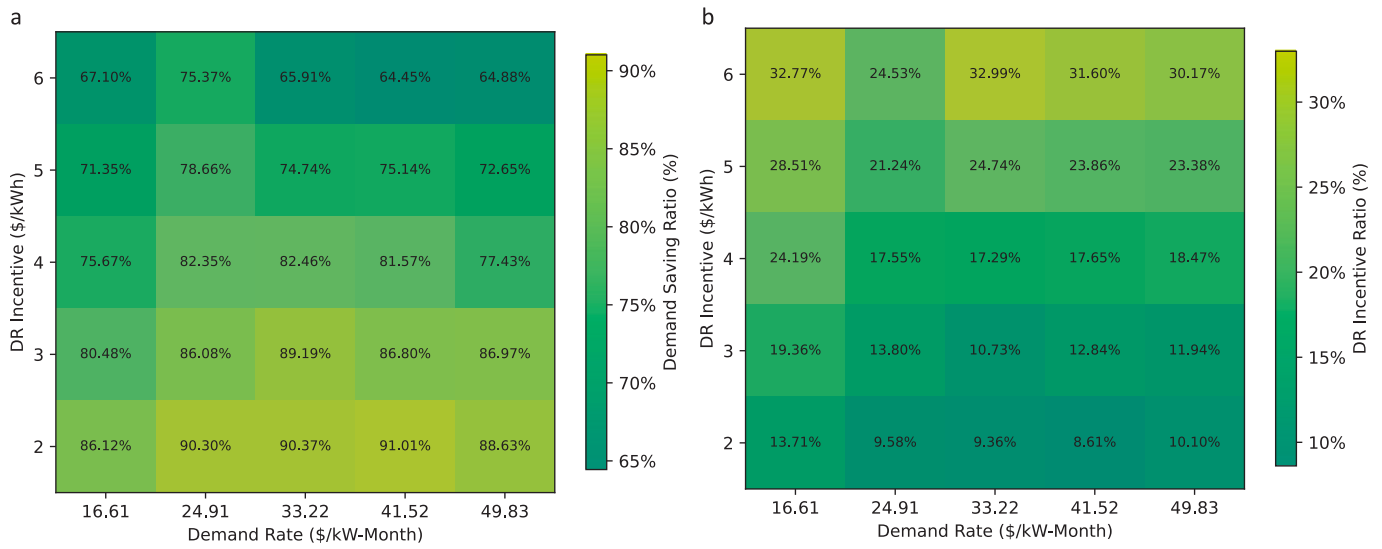

Fig. 11. The ratio of the a) demand saving and the b) DR incentive over the total saving.

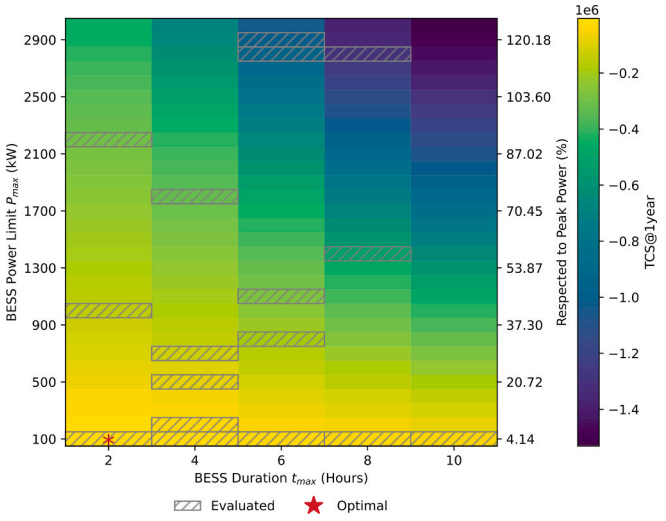

Fig. 12. The predicted TCS@1year for PS and power-reduction DR using the surrogate model.

reduction DR, with the power-reduction DR, the incentive will stop increasing once the duration increases from 6 h to 8 h. This is because the committed power, $P^{BESS,DR}$, reaches the P_{max} limit. A BESS with short duration is favored by the proposed methods. As the duration increases from 2 h to 8 h the total saving increases by 82.46 % while the BESS cost increases by 186.93 %. As the duration increases, the increased capacity is not fully utilized while still undergoes degradation. Interestingly, a BESS with a high P_{max} is not preferred. Even though more demand saving and incentive for DR can be collected with a high $P_{max,}$ as shown in Fig. 13b. The saving increases from $21,013 to $ 241,817. However, the BESS cost increased faster, from $25,771 to $529,995. The reason is similar to the PS only scenario. The degradation caused by the excessive cycle outnumbers the increased economic benefit of the PS and power-reduction DR. The excessive cycle increases the loss of active Li-ion from 8 mAh/cell to 57 mAh/cell. As for the savings, unlike the PS only scenario in which the savings only increase from $17,451 to $146,802 with P_{max} increases from 100 kW to 2200 kW, the savings increase at a faster rate from $21,013 to $241,817. Because the incentive collected from the power-reduction DR is directly related to the size of the BESS. However, the increased savings cannot match the increased cost. Therefore, the proposed method tends to select the smallest size with an NPV of $122,486, an EAA of $12,411/year, and an IRR of 18.34 %. Compared to PS only and PS with energy-reduction DR, PS with participation in power-reduction DR offers better economic benefit than the other two scenarios.

The same sensitivity analysis was performed. The optimal size in each scenario is presented in Fig. 14. As the demand rate and incentive increase, the proposed method tends to increase the P_{max} or/and t_{max} to capture more economic benefit. ANOVA is conducted on the optimal P_{max}. The analysis reveals that for the P_{max}, the demand rate is a dominant factor corresponding to the result that, for most of the scenarios, the demand saving accounts for more than 50 % of the total savings, as shown in Fig. 15a. With the original demand rate, as the incentive increases, the BO-MILP tends to select a BESS with a longer duration, and the same P_{max} results in a larger capacity, which can capture more incentive. Once the incentive increases from $200/kW-Year to $250/kW-Year, due to a larger capacity, the ratio between the incentives and total savings increases from 27.52 % to 45.57 %. A similar step change can be observed with the demand rate at $24.91/kW-Month once the incentive rate increases from $150/kW-Year to $200/kW-Year. However, even if the incentive and demand rate are high enough, proposed methods will always choose a BESS with P_{max} at 1900 kW. This behavior can be explained by Fig. 15c which shows the ratio of P_{max} and peak demand. Unlike the energy-reduction DR program, the power-reduction DR program focuses on the reduced power that must last at most 4 h. A proper P_{max} needs to be selected to serve both PS and power reduction. For site A, 1900 kW is around 78.84 % of the average peak demand. According to the load profile, on average, only 38.14 % of the time has a power demand higher than 1900 kW. Therefore, increasing the P_{max} cannot justify the cost, leading to a saturation effect of 1900 kW. From the BESS's duration perspective, once the DR incentive and demand rate are high enough, the proposed algorithm will choose the 4 h duration. The electricity rate schedule and the power-reduction DR program can explain this. According to the electricity rate schedule in Table 1, most peak hours last less than or equal to 4 h. A BESS with 4 h duration is enough for PS. Moreover, for the selected power-reduction DR program, the utility company requires the power reduction to last at most 4 h. Therefore, given the same P_{max} a longer duration is unnecessary.

4. Conclusion

This study introduced a BO-MILP framework for degradation-aware

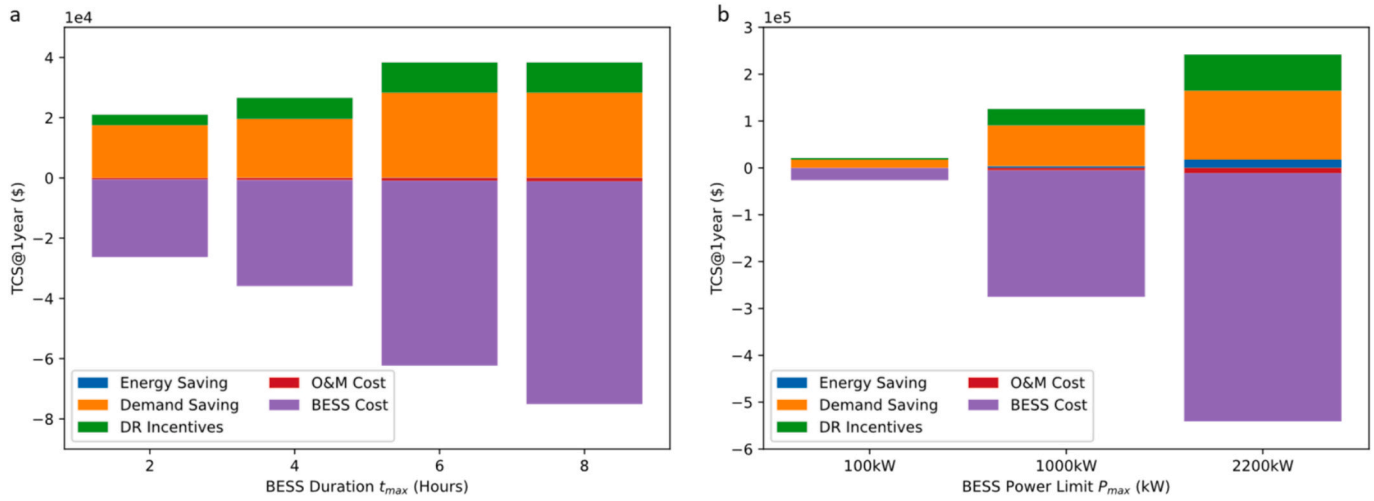

Fig. 13. a) The composition of TCS@1year for BESS with the same P_{max} at 100 kW but with durations ranging from 2 h to 8 h. b) The composition of TCS@1year for BESS with the same t_{max} at 2 h but with P_{max} ranging from 100 kW to 2200 kW.

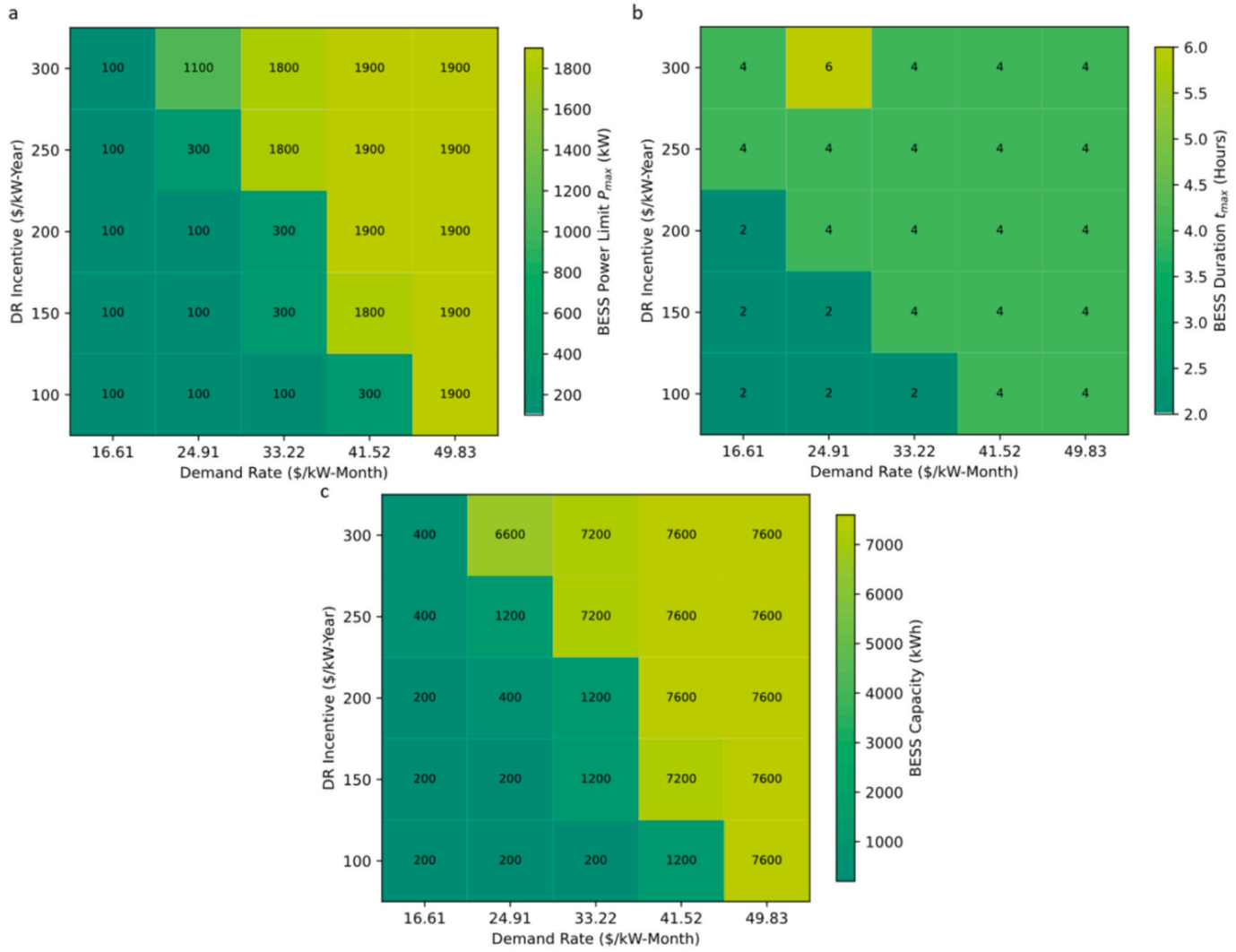

Fig. 14. The optimal a) P_{max}, b) t_{max}, and c) capacity are determined by the BO-MILP framework under different demand rates and DR incentives.

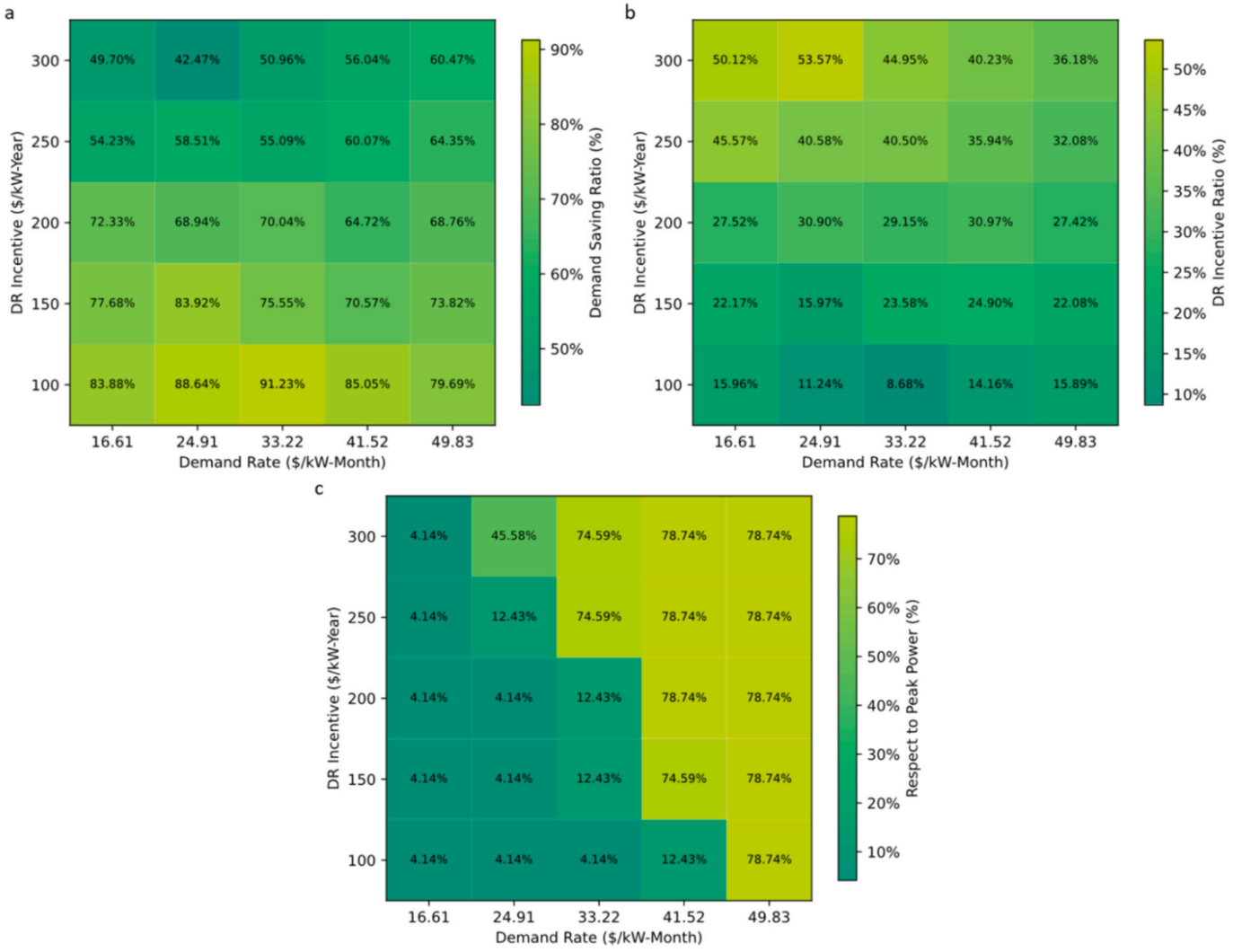

Fig. 15. The ratio of a) demand saving, b) DR incentive to total savings. The ratio of the P_{max} to peak power.

sizing of BESS participating in PS and DR programs. By coupling optimization with an electrochemical degradation model, the framework bridges economic and physical fidelity-identifying cost-optimal designs that remain durable under realistic cycling conditions. The results reveal that under current cost and rate structures, a minimal storage duration (2 hr) and 100 kW power capacities are most economical, but as demand rates or incentive levels rise, larger and longer-duration systems become favorable. These findings highlight a clear economic threshold for viable BESS investment and demonstrate how incentive design and rate structure affect the optimal storage size. Beyond quantitative optimization, the study offers following practical insights:

- System sizing depends on load characteristics and rate structures. Low load factors or high demand rates justify higher power limits, while high load factors favor smaller systems to avoid degradation.
- Stacking DR incentives with PS enhances profitability, though demand savings typically dominate under current pricing.
- Power-reduction DR participation yields the highest benefit among scenarios but is limited by program constraints on capacity and duration.

Looking ahead, incorporating stochastic and risk-aware formulations would enable investment decisions resilient to uncertain tariffs, load fluctuations, and DR participation. Load forecast uncertainty can influence both peakshaving performance and optimal sizing, and adding scenario-based or chance-constrained extensions would help make the framework more robust. Embedding degradation dynamics directly within the MILP could further align short-term operations with long-term health. The proposed BO-MILP framework thus not only informs optimal sizing and incentive design but also provides actionable heuristics—such as duration caps aligned with peak hours—that can guide industrial adopters and policymakers. Ultimately, this framework advances degradation-aware optimization from theoretical analysis toward a practical decision-support tool for accelerating BESS deployment and supporting the energy transition.

CRediT authorship contribution statement

Jiwei Yao: Writing – review & editing, Writing – original draft, Visualization, Validation, Methodology, Investigation, Formal analysis, Data curation, Conceptualization. **Blake Billings:** Writing – review & editing, Visualization, Supervision, Methodology, Investigation, Formal analysis. **Tao Gao:** Writing – review & editing, Visualization, Methodology. **John Hedengren:** Writing – review & editing, Visualization. **Kody M. Powell:** Writing – review & editing, Visualization, Supervision, Resources, Project administration, Formal analysis, Conceptualization.

Declaration of competing interest

The authors declare that they have no known competing financial interests or personal relationships that could have appeared to influence the work reported in this paper.

Acknowledgements

This work is funded by Utah Governor's Office of Energy Development [grant number 171881]; U.S. Department of Energy [grant number DE-EE0009708]. This manuscript has been authored in part by UT-Battelle, LLC, under contract DE-AC05-00OR22725 with the US Department of Energy (DOE). The publisher acknowledges the US government license to provide public access under the DOE Public Access Plan (http://energy.gov/downloads/doe-public-access-plan).

Data availability

Due to confidentiality agreements, the industrial load profiles used in this study cannot be made publicly available. However, interested readers may request access to the processed load profiles used in this work by contacting the corresponding author.

References

[1] Williams JH, Debenedictis A, Ghanadan R, Mahone A, Moore J, Iii WRM, et al. 2050 : the pivotal role of electricit. Science 2012;335:53–60.
[2] Semieniuk G, Taylor L, Rezai A, Foley DK. Plausible energy demand patterns in a growing global economy with climate policy. Nat Clim Chang 2021;11:313–8. https://doi.org/10.1038/s41558-020-00975-7.
[3] Dennis K, Colburn K, Lazar J. Environmentally beneficial electrification: the dawn of 'emissions efficiency. Electr J 2016;29:52–8. https://doi.org/10.1016/j.tej.2016.07.007.
[4] Stram BN. Key challenges to expanding renewable energy. Energy Policy 2016;96:728–34. https://doi.org/10.1016/j.enpol.2016.05.034.
[5] Benetti G, Caprino D, Della Vedova ML, Facchinetti T. Electric load management approaches for peak load reduction: a systematic literature review and state of the art. Sustain Cities Soc 2016;20:124–41. https://doi.org/10.1016/j.scs.2015.05.002.
[6] International Energy Agency. Integrating Solar and Wind Global experience and emerging challenges. 2024.
[7] Uddin M, Romlie MF, Abdullah MF, Abd Halim S, Abu Bakar AH, Chia KT. A review on peak load shaving strategies. Renew Sustain Energy Rev 2018;82:3323–32. https://doi.org/10.1016/j.rser.2017.10.056.
[8] Department of Energy. Demand Response n.d. https://www.energy.gov/oe/demand-response#:~:text=Demand response provides an opportunity,other forms of financial incentives.
[9] Chreim B, Esseghir M, Merghem-Boulahia L. Recent sizing, placement, and management techniques for individual and shared battery energy storage systems in residential areas: a review. Energy Rep 2024;11:250–60. https://doi.org/10.1016/j.egyr.2023.11.053.
[10] Antonio K, Mey A. US battery storage capacity expected to nearly double in 2024—US Energy information administration (Eia). EIA Moss Land Energy Storage Facil Accessed March 2024;24.
[11] Billings BW, Powell KM. Grid-responsive smart manufacturing: a perspective for an interconnected energy future in the industrial sector. AIChE J 2022;68. https://doi.org/10.1002/aic.17920.
[12] Billings BW, Smith PJ, Smith ST, Powell KM. Industrial battery operation and utilization in the presence of electrical load uncertainty using Bayesian decision theory. J Energy Storage 2022;53:105054. https://doi.org/10.1016/J.EST.2022.105054.
[13] Sanjari MJ, Karami H. Optimal control strategy of battery-integrated energy system considering load demand uncertainty. Energy 2020;210:118525. https://doi.org/10.1016/j.energy.2020.118525.
[14] Carpinelli G, di Fazio AR, Khormali S, Mottola F. Optimal sizing of battery storage systems for industrial applications when uncertainties exist. Energies 2014;7:130–49. https://doi.org/10.3390/en7010130.
[15] Hartmann B, Divényi D, Vokony I. Evaluation of business possibilities of energy storage at commercial and industrial consumers – a case study. Appl Energy 2018;222:59–66. https://doi.org/10.1016/j.apenergy.2018.04.005.
[16] Hannan MA, Faisal M, Jern Ker P, Begum RA, Dong ZY, Zhang C. Review of optimal methods and algorithms for sizing energy storage systems to achieve decarbonization in microgrid applications. Renew Sustain Energy Rev 2020;131:110022. https://doi.org/10.1016/j.rser.2020.110022.
[17] Chua KH, Lim YS, Morris S. Energy storage system for peak shaving. Int J Energy Sect Manag 2016;10:3–18. https://doi.org/10.1108/IJESM-01-2015-0003.
[18] Oudalov A, Cherkaoui R, Beguin A. Sizing optimal operation of battery energy storage system for peak shaving application. IEEE Lausanne POWERTECH Proc 2007;2007:621–5. https://doi.org/10.1109/PCT.2007.4538388.
[19] Leadbetter J, Swan L. Battery storage system for residential electricity peak demand shaving. Energ Buildings 2012;55:685–92. https://doi.org/10.1016/j.enbuild.2012.09.035.
[20] Lu C, Xu H, Pan X, Song J. Optimal sizing and control of battery energy storage system for peak load shaving. Energies 2014;7:8396–410. https://doi.org/10.3390/en7128396.
[21] Inaolaji A, Wu X, Roychowdhury R, Smith R. Optimal allocation of battery energy storage systems for peak shaving and reliability enhancement in distribution systems. J Energy Storage 2024;95:112305. https://doi.org/10.1016/j.est.2024.112305.
[22] Martins R, Hesse HC, Jungbauer J, Vorbuchner T, Musilek P. Optimal component sizing for peak shaving in battery energy storage system for industrial applications. Energies 2018;11. https://doi.org/10.3390/en11082048.
[23] Wankhade SD, Patil BR. Lithium-ion battery: battery sizing with charge scheduling for load levelling, ramp rate control and peak shaving using metaheuristic algorithms. J Energy Storage 2024;86:111223. https://doi.org/10.1016/j.est.2024.111223.
[24] Jin R, Song J, Liu J, Li W, Lu C. Location and capacity optimization of distributed energy storage system in peak-shaving. Energies 2020;13. https://doi.org/10.3390/en13030513.
[25] Ke BR, Ku TT, Ke YL, Chuang CY, Chen HZ. Sizing the battery energy storage system on a university campus with prediction of load and photovoltaic generation. 2015 IEEE/IAS 51st Ind Commer Power Syst Tech Conf I CPS 2015 2015:1–12. https://doi.org/10.1109/ICPS.2015.7266406.
[26] Hesse HC, Martins R, Musilek P, Naumann M, Truong CN, Jossen A. Economic optimization of component sizing for residential battery storage systems. Energies 2017;10. https://doi.org/10.3390/en10070835.
[27] Choi SS, Lim HS. Factors that affect cycle-life and possible degradation mechanisms of a Li-ion cell based on LiCoO2. J Power Sources 2002;111:130–6. https://doi.org/10.1016/S0378-7753(02)00305-1.
[28] Jülch V. Comparison of electricity storage options using levelized cost of storage (LCOS) method. Appl Energy 2016;183:1594–606. https://doi.org/10.1016/j.apenergy.2016.08.165.
[29] Shi Y, Xu B, Wang D, Zhang B. Using battery storage for peak shaving and frequency regulation: joint optimization for superlinear gains. IEEE Trans Power Syst 2018;33:2882–94. https://doi.org/10.1109/TPWRS.2017.2749512.
[30] Englberger S, Jossen A, Hesse H. Unlocking the potential of battery storage with the dynamic stacking of multiple applications. Cell Reports Phys Sci 2020;1:100238. https://doi.org/10.1016/j.xcrp.2020.100238.
[31] Shi Y, Xu B, Tan Y, Kirschen D, Zhang B. Optimal battery control under cycle aging mechanisms in pay for performance settings. IEEE Trans Automat Contr 2019;64:2324–39. https://doi.org/10.1109/TAC.2018.2867507.
[32] Padmanabhan N, Ahmed M, Bhattacharya K. Battery energy storage systems in energy and reserve markets. IEEE Trans Power Syst 2020;35:215–26. https://doi.org/10.1109/TPWRS.2019.2936131.
[33] Keil P, Schuster SF, Wilhelm J, Travi J, Hauser A, Karl RC, et al. Calendar aging of lithium-ion batteries. J Electrochem Soc 2016;163:A1872–80. https://doi.org/10.1149/2.0411609jes.
[34] Zhang Y, Anvari-Moghaddam A, Peyghami S, Li Y, Dragičević T, Blaabjerg F. Optimal sizing of behind-the-meter battery storage for providing profit-oriented stackable services. IEEE Trans Smart Grid 2024;15:1481–94. https://doi.org/10.1109/TSG.2023.3292076.
[35] Peng P, Li Y, Li D, Guan Y, Yang P, Hu Z, et al. Optimized economic operation strategy for distributed energy storage with multi-profit mode. IEEE Access 2021;9:8299–311. https://doi.org/10.1109/ACCESS.2020.3047230.
[36] Elio J, Milcarek RJ. A comparison of optimal peak clipping and load shifting energy storage dispatch control strategies for event-based demand response. Energy Convers Manag X 2023;19:100392. https://doi.org/10.1016/j.ecmx.2023.100392.
[37] Frazier PI. A Tutorial on Bayesian Optimization 2018:1–22.
[38] Elio J, Phelan P, Villalobos R, Milcarek RJ. A review of energy storage technologies for demand-side management in industrial facilities. J Clean Prod 2021;307:127322. https://doi.org/10.1016/j.jclepro.2021.127322.
[39] United State Bureau of Labor Statistics. Consumer Price Index n.d. https://www.bls.gov/cpi/home.htm.
[40] Viswanathan V, Mongird K, Franks R, Li X, Sprenkle V, Baxter R. Grid energy storage technology cost and performance assessment 2022:151.
[41] Yang XG, Leng Y, Zhang G, Ge S, Wang CY. Modeling of lithium plating induced aging of lithium-ion batteries: transition from linear to nonlinear aging. J Power Sources 2017;360:28–40. https://doi.org/10.1016/j.jpowsour.2017.05.110.
[42] Yao J, Gao T, Hedengren J, Powell KM. Maximizing the benefit of industrial battery energy storage through incentive stacking and optimal dispatch. Available SSRN 5152257 n.d.
[43] California Public Utilities Commission. Emergency Load Reduction Program n.d. https://www.cpuc.ca.gov/industries-and-topics/electrical-energy/electric-costs/demand-response-dr/emergency-load-reduction-program.
[44] Rocky Mountain Power. Demand Response n.d. https://www.rockymountainpower.net/savings-energy-choices/business/demand-response.html.
[45] CAISO. Grid Emergencies History Report. n.d.
[46] Rocky Mountain Power. Demand Response. Demand Response n.d. https://www.rockymountainpower.net/savings-energy-choices/business/demand-response.html.